Supplementary Notes

February 1, 2007

Contents

1 Appendix A. The seasonally forced SIR Model

The classical SIR model with vital rates takes the following form:

$$\begin{aligned} \dot{S} &= \mu N - \mu S - \beta(t) SI/N \\ \dot{I} &= \beta(t) SI/N - \gamma I - \mu I \\ \dot{R} &= \gamma I - \mu R. \end{aligned} \tag{1}$$

where S, I and R are the number of Susceptibles, Infectives and Recovered individuals in the population respectively. It is assumed that all classes of the population reproduce and die at the same per-capita rate μ. The parameter γ represents the rate at which infected individuals recover. $\beta(t)$ is defined as the contact rate between infected and susceptible individuals. The rate is assumed to follow the classical 'Law of Mass Action' in which the rate of interaction of S and I is proportional to the product SI, as would be expected under homogeneous mixing conditions.

Note that for all time the population size $S + I + R = N$ is constant ($\dot{S} + \dot{I} + \dot{R} = 0$). Thus it is only necessary to work with the two first equations describing the rates for S and I in (1). It is convenient to set the total population size to $N = 1$ and the variables S, I, and R might then be viewed as proportions of the entire population.

In simulations, we follow [1,2] and incorporate a small amount of immigration every year, that helps reduce the population variability generated by the forced model, especially the large "troughs and valleys" between epidemics. This is achieved by rewriting the mass action term SI in Eqns. (1) as $S(I + \epsilon)$ where the small immigration term is $\epsilon = 10^{-12}$ (see Methods, main text). Other immigrations schemes have been tested and yield similar results. In fact, all theoretical results reported here have no dependence on the presence or absence of immigration. Further reduction in variability may be effectively achieved by incorporating sinusoidal forcing rather than the Hi-Lo step-function.

For childhood epidemics such as measles, chickenpox and mumps the contact rate (β) shows substantial seasonal variation[4,5,7,9] whereby some periods of the year have environmental conditions more suitable for infection than others. The high contact rates amongst children at the beginning of the school year in winter strongly facilitates transmission of disease. To incorporate seasonality in a simple yet effective fashion, we assume that there are only two seasons in each year and the transmission rate is:

$$\beta(t) = \begin{cases} \beta^+ = \beta_0(1+\delta) & \mathbf{H}igh\ season \\ \beta^- = \beta_0(1-\delta) & \mathbf{L}ow\ season \end{cases} \tag{2}$$

where β_0 gives the mean contact rate and $0 < \delta < 1$ represents the strength of the seasonal forcing modulating the contact rate. Over time the seasons change sequentially $H \rightarrow L \rightarrow H \rightarrow L$.....

The sharp difference between High and Low seasons has similarities to that observed in contact rate studies of the USA data which has been estimated to be roughly sinusoidal[9] ($\beta(t) = \beta_0(1 + \delta sin(2\pi t))$) although the transition between seasons is more continuous/gentle. Our results also hold with sinusoidal forcing; in particular the threshold described in the text is equally as relevant (details upon request). Nevertheless, we stay with the two season framework, which makes the mathematical analysis tractable.

The UK data, has school term-time forcing with longer winter periods (HI season) interspersed with holiday breaks (LO)[4,5]. As an approximation, rather than only setting the High season as 50% of the year (as in simulations of Fig.2 main text), we also explored cases of 60%, 70%, 80% and achieved similar results. We have also incorporated the full term-time forcing detailed in Keeling et al. (7).

As displayed in the time series of infected reported cases of measles in the pre-vaccination era, many cities in the United Kingdom and the United States are characterized by 'skips' (see Fig.1 in main text). That is, in a number of years, major epidemics do not appear to take place at all.

1.1 The outbreak and the susceptible buildup regimes

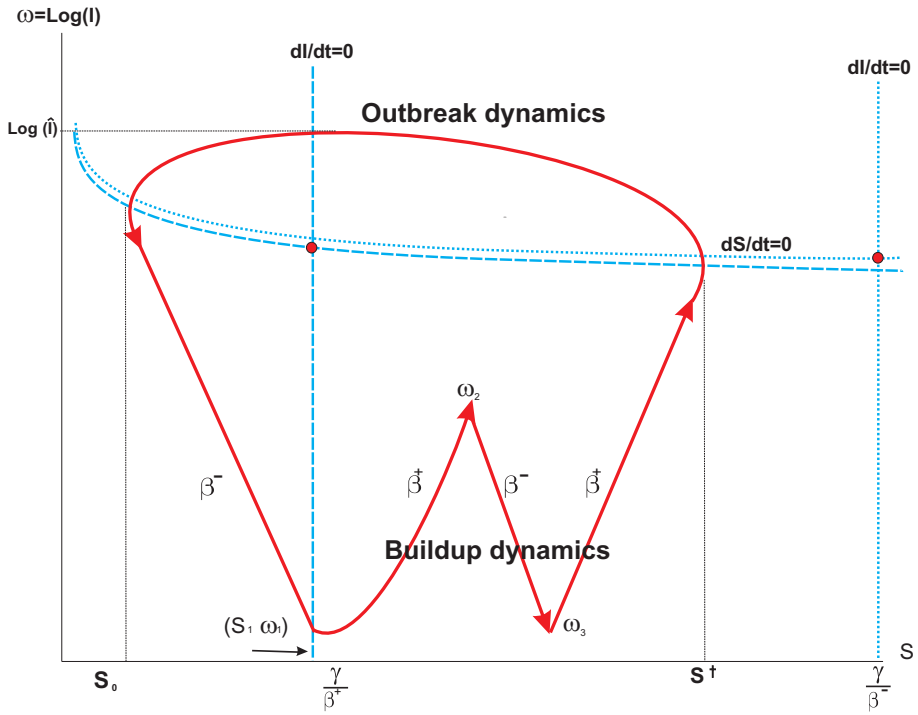

Figure 1: Phase plane diagram with infectives (log I) plotted as a function of susceptible numbers (S). The SIR model's (1) trajectory rotates counter-clockwise around the phase plane. The trajectory is attracted to the quasi-equilibrium associated with each season (the null-cline intersection, red circles). As the season (and contact-rates $\beta^{+/-}$) change, the trajectory is kicked from one equilibrium to the next.

It is helpful to study the dynamics of the model in the phase plane portrait of Fig.1. The plot of I versus S shows the trajectory of model (1) as it rotates counter-clockwise around the *phase plane*. In the two-season approximation each season (in which β is constant) has its own corresponding attracting equilibrium point. As the seasons change, the trajectory is attracted to the "quasi-equilibrium" associated with each season (see circles marked in Fig.1). Non-equilibrium behaviour arises as the trajectory is kicked away from one equilibrium to the next (see also Keeling et al. 2001).

The phase-plane may be divided into an upper and lower section as shown in Fig. 1. We will say more about the dividing line, the S-nullcline, shortly. Trajectories in the upper part correspond to the epidemic's fast outbreak dynamics where infectives increase to very large numbers and then crash. Trajectories confined to the lower part correspond to a regime in which there is a slow build up of susceptibles accumulating (due to births) in the absence of a large-scale epidemic. Following the solution trajectories as they wind around the phase plane and cross from one regime to the other allows us to capture the full dynamics as the model solution changes from season to season.

More accurately each season has its associated S nullcline curve defined as:

$$dS/dt = \mu(1-S) - \beta^{\pm} IS = 0 \tag{3}$$

namely:

$$I = \frac{\mu(1-S)}{S\beta^{\pm}} \simeq \frac{\mu}{S\beta^{\pm}} \tag{4}$$

The approximation above is based on the fact that for most infectious diseases applications $\mu \ll \beta$ (for measles, $\mu = 0.02$ and $\beta = 1600$). Also note that for realistic parameters, the two nullclines lie very close

to one another as shown in Fig.1. This is because in Fig.1 the model solution $I(t)$ ranges through six or more orders of magnitude (as in real populations of large cities) setting the scale of the vertical axis of the graph. However, the variability in the nullcline I induced by β (via changes in δ) in Eqn.4 is of the order of a factor of $(1+\delta)$. Thus I might change by $\approx 30\%$ for $\delta = 0.3$ (considered relatively large). Thus the changes reflected in the two nullclines are relatively small compared to the orders of magnitude changes in $I(t)$, and they appear almost identical

1.2 Fast Epidemic Dynamics

During a major epidemic, the mortality and birth rate terms μ in (1) are relatively small and have little influence on the dynamics. Thus when $I \gg \frac{\mu}{S\beta^{\pm}}$ (above the S null-cline) it is possible to approximate (1) as:

$$\begin{aligned} \dot{S} &= -\beta(t)SI \\ \dot{I} &= I\,(\beta(t)S - \gamma - \mu). \end{aligned} \tag{5}$$

Let $(S, I) = (S^{\dagger}, I^{\dagger})$ be the entry point to the outbreak regime at time $t^{\dagger}$ (see Fig.1). Since the entry point occurs on the S-nullcline to equation (1) then $I^{\dagger} = \frac{\mu}{\beta S^{\dagger}}$ (see equation 4.

Following Kermack and McKendrick (1927) it is possible to approximate $S(t)$, $I(t)$ and $R(t)$ analytically for a given value of β. In particular, for infectives:

$$I(t) = \frac{1}{\gamma}\dot{R(t)} = \frac{\sigma^2\gamma^2}{2\beta^2 S^{\dagger}}\mathrm{sech}^2(\frac{1}{2}\sigma\gamma t - \phi) \tag{6}$$

where

$$\sigma^2 = (\frac{\beta S^{\dagger}}{\gamma} - 1)^2 + \frac{2\beta^2 S^{\dagger} I^{\dagger}}{\gamma^2}, \;\; \phi = \mathrm{a}tanh[\frac{1}{\sigma}(\frac{\beta S^{\dagger}}{\gamma} - 1)], \tag{7}$$

Since $t^{\dagger}$ is the time of entry to the outbreak regime, it is easy to see that $I(t)$ obtains its maximal value

$$\hat{I} = \frac{\sigma^2\gamma^2}{2\beta^2 S^{\dagger}} \tag{8}$$

at time $t = \frac{2\phi}{\sigma\gamma} + t^{\dagger}$.

Thus the time of year the number of infectives reach a maximum, i.e., the phase, is directly related to the time of entry $t^{\dagger}$. This is a property referred to in the main text of our paper.

The outbreak dynamics ends at $t = t_0$ where the trajectory crosses once again the S null-cline at coordinates (S_0, I_0).

1.3 Slow buildup dynamics

When $I \ll \frac{\mu}{\beta^{\pm} S}$, that is after the trajectory has fallen below the S null-cline, then (1) may be approximated as :

$$\begin{aligned} \dot{S} &= \mu \\ \dot{I} &= I\,(\beta(t)S - \gamma - \mu). \end{aligned} \tag{9}$$

with initial conditions for these equations being (S_0, I_0) (see Fig.1).

The rate of change of S is slow for the buildup solutions compared to the very fast changes experienced during an outbreak. Therefore, the system spends most of its time in the buildup regime below the S null-cline. In the next section we approximate the solution to this system of equations (9).

2 Appendix B. Determining the Number of Skips as a Function of S_0

A skip is the absence of an outbreak that would normally be expected in the High Season. Skips necessarily occur in the lower half of the phase plane (see Fig.1) and their dynamics are described to a good approximation by equations (9). We proceed to study these further. Recall that a year is taken to have only two seasons. It starts in the Low season at times $t_n, \quad n = 0, 2, 4, ..$ with a low infection rate $\beta^- = \beta_0(1-\delta)$ and lasts for a time interval $p * \tau = T^-$, where τ is the period length (i.e a year) and $0 < p < 1$. This is followed by the High season at times $t_n, \quad n = 1, 3, 5, ..$ with high infection rate $\beta^+ = \beta_0(1+\delta)$, which lasts for $(1-p) * \tau = T^+$.

The overall strategy for solving system (9) is to calculate the solution in the time intervals between t_n and t_{n+1}. Each time interval will have a constant infection rate (i.e. either β^+ or β^-) and initial values S_n and I_n. The scheme stops whenever $I_n = \frac{\mu}{\beta S}$ which is the S null-cline curve in the (I, S) phase plane. At this point we return back to the outbreak solutions (6).

We define a point where the infected population reaches a local maximum I_m and which lies below the S null-cline as a skipping point. These minor outbreaks arise because the trajectory is curtailed in the phase plane due to a change of season and are prevented from ever triggering a large amplitude epidemic. The difference between a skipping point and an epidemic peak is not just a question of magnitude. As the trajectory passes through a skipping point the susceptible population **always** continues to **increase** despite the fact that the number of infectious individuals pass through a maximum. In contrast, as the trajectory passes through an epidemic peak, the susceptible population **declines**. This provides a natural topological criterion to distinguish between a 'skip' and an outbreak.

We first scale susceptibles and infectives so that $s = \frac{\beta_0}{\gamma+\mu} S$ and $w = \log I$. An equivalent system to (9) is:

$$\begin{aligned} \dot{s} &= m \\ \frac{\dot{w}}{\Gamma} &= (1 \pm \delta)s - 1 \end{aligned} \tag{10}$$

where $m = \frac{\beta_0 \mu}{\gamma+\mu}$ and $\Gamma = \gamma + \mu$.

Observe that the susceptibles are always increasing with a constant rate m:

$$s(t) = mt + c_0 \tag{11}$$

where $c_0 = s_0 - mt_0$. From the phase plane (Fig.1) we see that (s_1, w_1) is a sharp point that results from the change of $\beta(t)$ as it jumps from β^- to β^+. All sharp points (s_n, w_n) are produced by this mechanism. By integrating system (10) between two neighboring sharp points and assuming that t_0 occurs during the low season ($\beta(t) = \beta^-$) it is possible to obtain recursive algebraic expressions for $\omega_0, \omega_1, \omega_2 ...., \omega_n$ (see Olinky (2005), Olinky et al. (2007))

As mentioned previously, the s nullclines in the phase plane are similarly positioned and in the region of the attractor may be approximated as a horizontal line for realistic parameters. Thus this recursive scheme stops whenever $w_n > \log(\frac{m}{\beta^{\pm} s}) \approx w_0$.

Let us define $\hat{n}$ to be the smallest n where $w_n > \log(\frac{m}{\beta^{\pm} s}) \approx w_0$, then the overall number of skips is given by $k \approx [\frac{\hat{n}}{2}] - 1$ where $[x]$ is the integer value of x. Based on the recursive expressions for the ω_i,

and recalling that $\hat{n} \approx 2(k+1)$, this can be written in terms of s_0 as:

$$s_0 > 1 - \frac{m\tau}{2}(k+1) - \frac{\delta m\tau}{8(k+1)} \tag{12}$$

Changing back to the natural variables ($s = \frac{\beta_0}{\gamma+\mu}S$ and $m = \frac{\beta_0\mu}{\gamma+\mu}$) we arrive at:

$$S_c(k) = \frac{\gamma+\mu}{\beta_0} - \frac{\mu\tau}{2} * (k+1) - \frac{\delta\mu\tau}{8(k+1)}. \tag{13}$$

where $\tau = 1$ year. For the parameters of most disease dynamics the very last term ($\delta\mu$) is of small magnitude and may be neglected. Similarly, $\mu \ll \gamma$. Then $S_c(k)$ acts as a threshold such that:

• if $S_0 > S_c(k)$ the trajectory must continue on to have less than or equal to k consecutive skips in the coming years.

• if $S_0 < S_c(k)$, the trajectory must be greater than k consecutive skips in the coming years.

Intensive numerical simulations coincide with the threshold approximation given above. See for example Fig.3 of main text. In testing the threshold peaks we equivalently determined intervals between major epidemics by calculating the time between consecutive minima in sussceptible numbers i.e. time between successive minima.

As mentioned in the main text the seasonally forced SIR model is used in a range of applications from studies of influenza dynamics to models of plant pathogens as agents of bioterrorism. The threshold identified above should have importance in many of these different contexts. The same principles may also be of value in seasonally forced models of biological populations helping, say, identify phase switching effects ("chicken steps") seen in the Tribolium studies of Henson et al. (1998) [13]. Further work is needed to extend Henson et. al's study to include forcing.

3 Appendix C. Intuitive Interpretation of the Threshold

Insights regarding the importance of S_0, the formula for the threshold and the number of skips can be gained by analysing the model's orbit in the absence of forcing ($\delta = 0$). The rather simple analysis is in fact very revealing. Consider the dynamics in the lower phase plane when $\delta = 0$ (10):

$$\frac{\dot{w}}{\Gamma} = s - 1 \tag{14}$$

where $s(t) = mt + s_0$.

This has solution:

$$w(t) = \Gamma t(mt/2 + s_0 - 1) + w(0). \tag{15}$$

Recall that s_0 and w_0 are initial conditions that begin on the S-nullcline, the entry point to the lower-half of the phase plane. The above solution for $w(t)$ describes a parabola in the $w-t$ plane, with $w(t)$ descending and then increasing (i.e., passing through a minimum) with time. Following the logic used in Appendix B, we seek the value of t where $w(t)$ reaches $w(0)$. This approximates the model's recovery time between epidemics (similar to the time the trajectory spends in the lower half of the phase plane in Appendix B.) It occurs when $W(t) = t(mt/2 + s_0 - 1) = 0$. Now $W(t) = 0$ has roots at $t_0 = 0$ and $t_1 = 2(1 - s_0)/m$.

The model's recovery time between epidemics may be approximated as the time the trajectory spends between t_0 and t_1, namely, $t_1 - t_0 = 2(1 - s_0)/m$ years.

The number of skips is $k \simeq 2(1-s_0)/(m\tau) - 1$.

Thus we obtain $s_0 \simeq 1 - m(k+1)\tau/2$ as the critical s_0, giving the same threshold as found for the forced system. After returning to original variables ($s = \frac{\beta_0}{\gamma+\mu} S$ and $m = \frac{\beta_0 \mu}{\gamma+\mu}$) we arrive at:

$$S_c \simeq \frac{\gamma+\mu}{\beta_0} - \frac{(k+1)\mu\tau}{2}. \tag{16}$$

The relationship of the $\delta = 0$ scenario to the full forced model, and the implications of R_0 are discussed in further detail in Olinky et al. (2007).

4 Appendix D. Peak versus Phase relationship derived via Phase Plane Analysis

Here we use the power of phase plane analysis to show why the phase relationship established in the paper must hold. Consider an ensemble of trajectories that all originate from the same point $(S^\dagger, I^\dagger)$ (see Fig. 2) but are initiated at different phases θ (month of year). In the absence of a seasonal change, these trajectories would all reach the same maximum level $\hat{I}$, but at different phases. In the absence of a seasonal change at the end of the epidemic all trajectories reach the same terminal number of susceptibles, say, S_a.

Suppose now that there is a seasonal change while the epidemic is in progress. This might happen if the trajectory is initiated relatively late in the season; hence it will also peak late in the season (i.e. closer to the seasonal change). For these outbreaks a change in β to the Low season will have the effect of curtailing the trajectory (see Fig. 2).

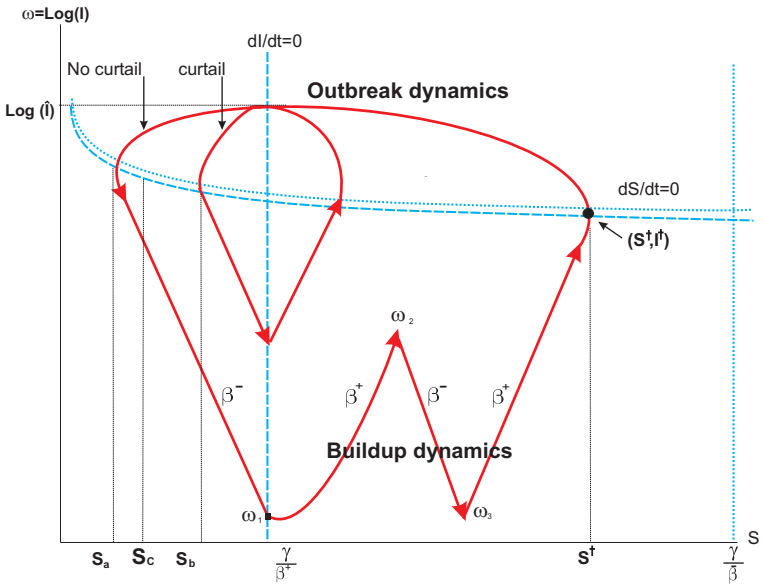

Figure 2: Phase plane diagram with infectives (log I) plotted as a function of susceptible numbers (S). The SIR model's (1) trajectory rotates counter-clockwise around the phase plane. The figure shows schematically how a skip is triggered if $S < S_c$ or an outbreak if $S > S_c$.

As a result, the epidemic decline is enhanced resulting in a larger pool of susceptibles $S_b > S_a$ at the crossing of the S null-cline. Thus, **the later the outbreak peaks, the larger the susceptible level** S_0. An interesting case occurs when $S_a < S_c < S_b$. Here $S_c = S_c(0)$ is the threshold for skips. It implies that curtailing due to seasonal change increases S_b beyond the threshold S_c and inhibits the skip, resulting in an

outbreak, as shown in Fig. (2).

5 Appendix E. TSIR Model

The phase relationship obtained for the deterministic (chaotic) SIR model also occurs in stochastic epidemic models. We demonstrate this using the Time-Series SIR model, or so called TSIR model[3,6]. In Fig.5 we show the outcome of a simulation of the TSIR (Eqn, 17) where, as usual, we plot the peak height of the next year's epidemic as a function of the phase of the current year. The deterministic SIR forced model yields a similar phase relationship (see Fig.4 (main text)).

The TSIR model is based on the equations:

$$\begin{aligned} S_{t+1} &= S_t + B_t - I_{t+1} \\ \lambda_{t+1} &= \beta_s (I_t + \theta_t)^{\alpha} (S_t)^{\gamma}. \end{aligned} \tag{17}$$

$I_{t-1} \sim NB(\lambda_{t+1}, I_t)$. where $NB(\lambda_{t+1}, I_t)$ signifies a negative binomial process, with expectation λ_{t+1} and clumping parameter I_t, see[3,6] for further details. Similar to [3,6] we used the following parameters $\alpha = 0.97$, $B_t = 900$,$\gamma = 1$ and ϕ_t follows a Poisson process with time-invariant mean m (m=0.2). To incorporate seasonality in a simple yet effective fashion, we assume that there are only two seasons in each year using Eqn. (2) as done for the SIR model. In the simulation the high season ($\beta^+ = 3.6 \cdot 10^{-5}$) is 36 weeks (to mimic the extended winter of the UK) while the remaining 16 weeks ($\beta^- = 2.1 \cdot 10^{-5}$). These magnitudes are similar to those found in [3,6]. The simulation results are similar if the High and Low seasons are each 26 weeks.

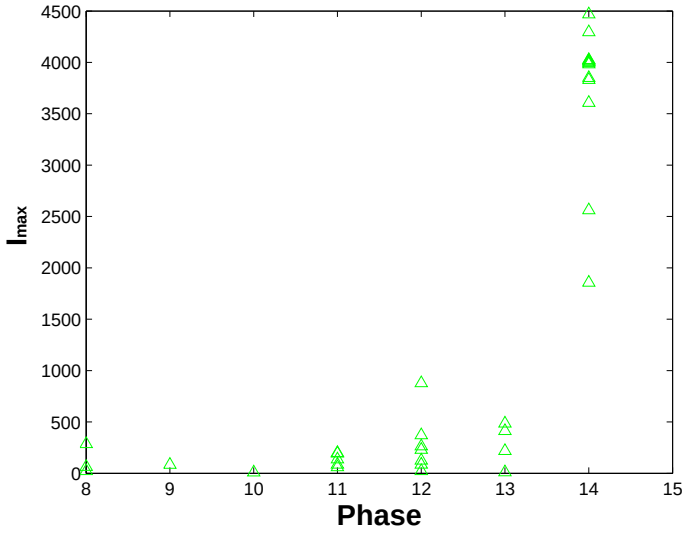

Figure 3: .The relationship between an outbreak's *current phase* and the maximum number of infectives in the *following year's* outbreak in a stochastic (TSIR) model.

The TSIR model also has a **threshold** that depends critically on S_0 that divides annual dynamics from biennial as shown in the Fig. (4) below (cf. Fig.4 of main text). Using the TSIR model with term-time forcing as detailed exactly in[11] leads to similar results as in Fig. (4).

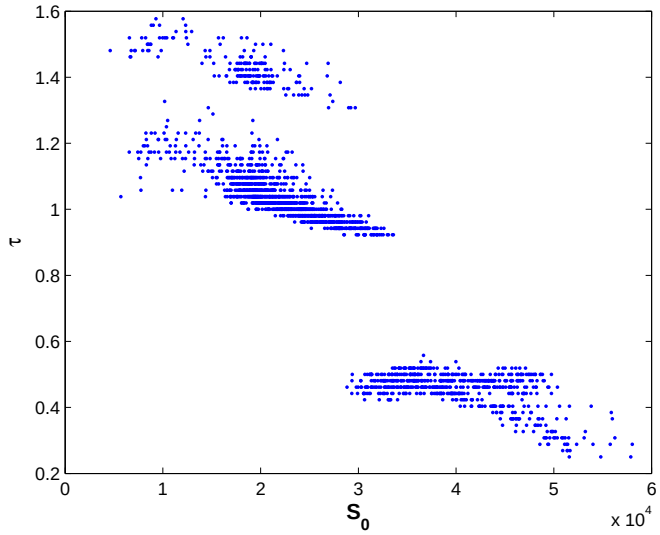

Figure 4: . A simulation of a stochastic (TSIR) model. The time τ between two successive large-scale epidemics, is plotted as a function of the susceptibles S_0 left in the wake of the first epidemic.

6 Appendix F. Data analysis & Phase relationship

Figure 5 plots all four time series used to derive the phase-relationship of figure 4 in the main text. We first identified all possible maxima in the time series. Given the weekly resolution of the UK time series, it proved helpful to smooth the data using a Gaussian kernel. (Smoothing made little difference to peak-detection in the US data largely due to its monthly resolution.) Recall that the phase-relationship is a plot of the number of next year's infectives as a function of the phase of this year's *major outbreak*. Skips are therefore not required as "predictees" and are omitted from the analysis. For the UK and US measles time series, skips comprise some 30% and 50% of the datapoints respectively. Likewise, due to the action of the threshold, the very largest peaks (independent of their phase) were always followed by skips, and hence were also removed from the analysis. In practice we removed the largest epidemic found in each time series, although the results obtained were robust to inclusion of these latter points.

Figure 7 gives a detailed breakdown of exactly those points (marked with a $\star$) used to compute the phase relationship. The final datasets were comprised of intermediate size epidemic peaks with cases of infectives in the ranges: Birmingham (230-2,500), London (500-4,500), Baltimore (cases:400-5,000), and New York measles (4,000-12,000).

To show the robustness of the phase relationship, the analysis was repeated for other large cities in the UK: Sheffield, Newcastle, Manchester, and Bristol (data from http://www.zoo.ufl.edu/bolker). The resulting plots are given in Fig. 6.

The phase-relationship was also checked in the New York mumps time series (1928-1972, see fig.(7 inset.) As the theory suggests, the relationship is best viewed when analysing epidemics of roughly the same size. There are no skips in the time series, which makes more data available for this type of analysis. We Intermediate peak heights in the range (700:1050) (see Fig.7 inset) were chosen to study the effect of phase. Because some of the peaks were difficult to detect, the time-series was smoothed using a Gaussian kernel.

The epidemic outbreaks have little variability in phase and mostly occur in months 4 or 5. Nevertheless outbreaks peaking in month 4 (April) are, on average, followed by much smaller epidemics than those peaking in month 5. This corresponds with the hypothesised expectation for the phase relationship.

In Figure 1d) main text, the phase of the peak in 1962 was impossible to estimate and the datapoint was dropped from the analysis.

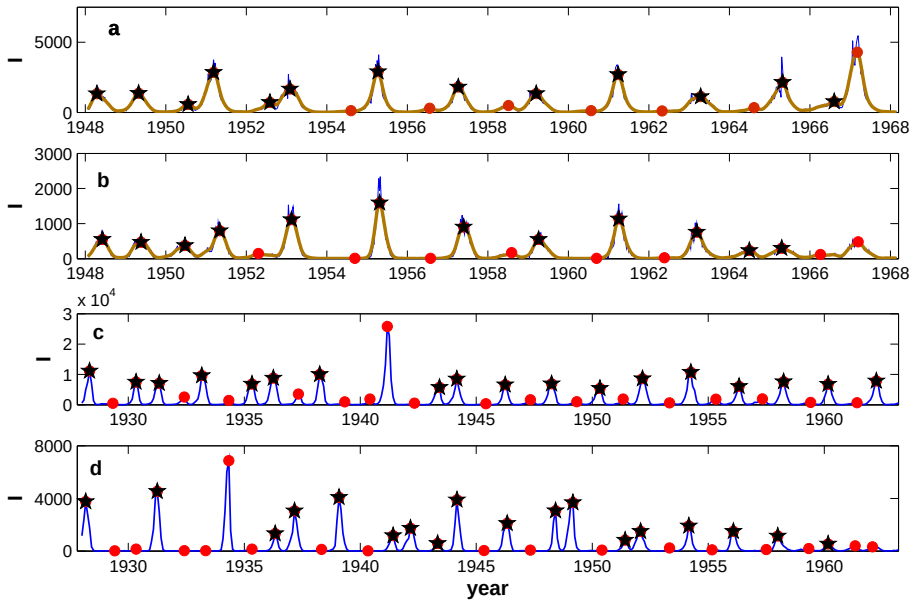

Figure 5: Time series of reported measles infective cases in the pre-vaccination era from a) London b) Birmingham c) New York d) Baltimore. The symbol "⋆" indicates peaks that were used as part of the phase analysis, while the symbol "•" indicates those peaks that were excluded.

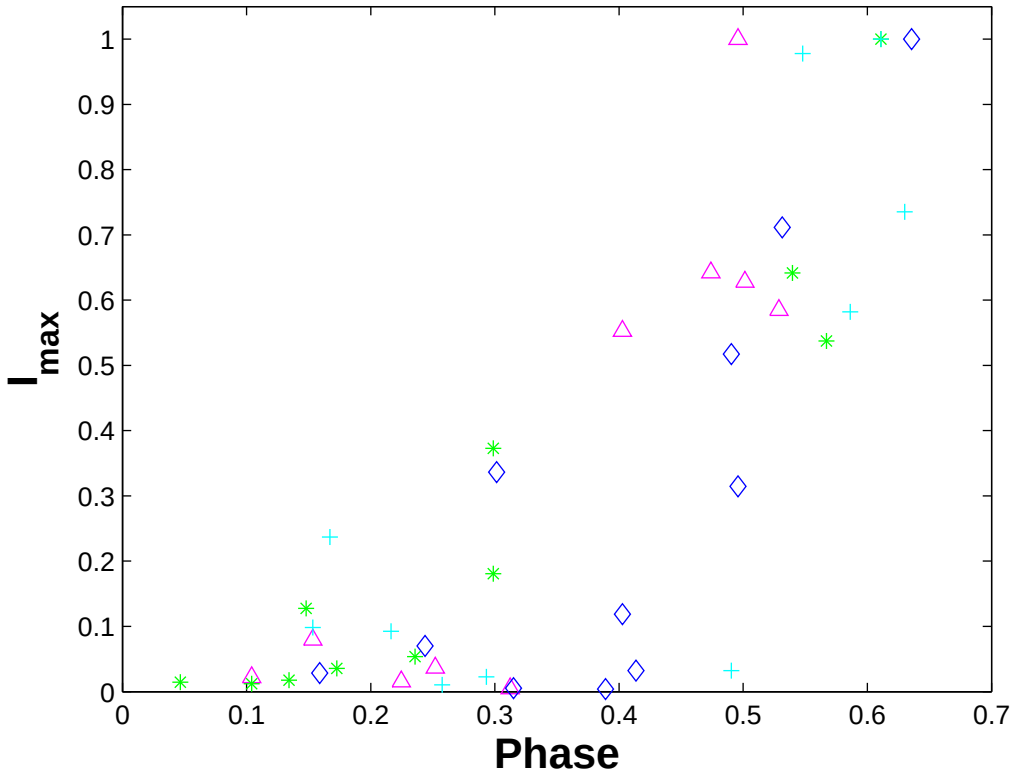

Figure 6: The relationship between an outbreak's *current phase* and the maximum number of infectives in the *following year's* outbreak (data from http://www.zoo.ufl.edu/bolker/). All intermediate sized epidemic peaks were collected in the ranges specified: Sheffield (+ 100:400), Newcastle (△ 130:300), Manchester (∗ 150:600), and Bristol(♢ 100:500).

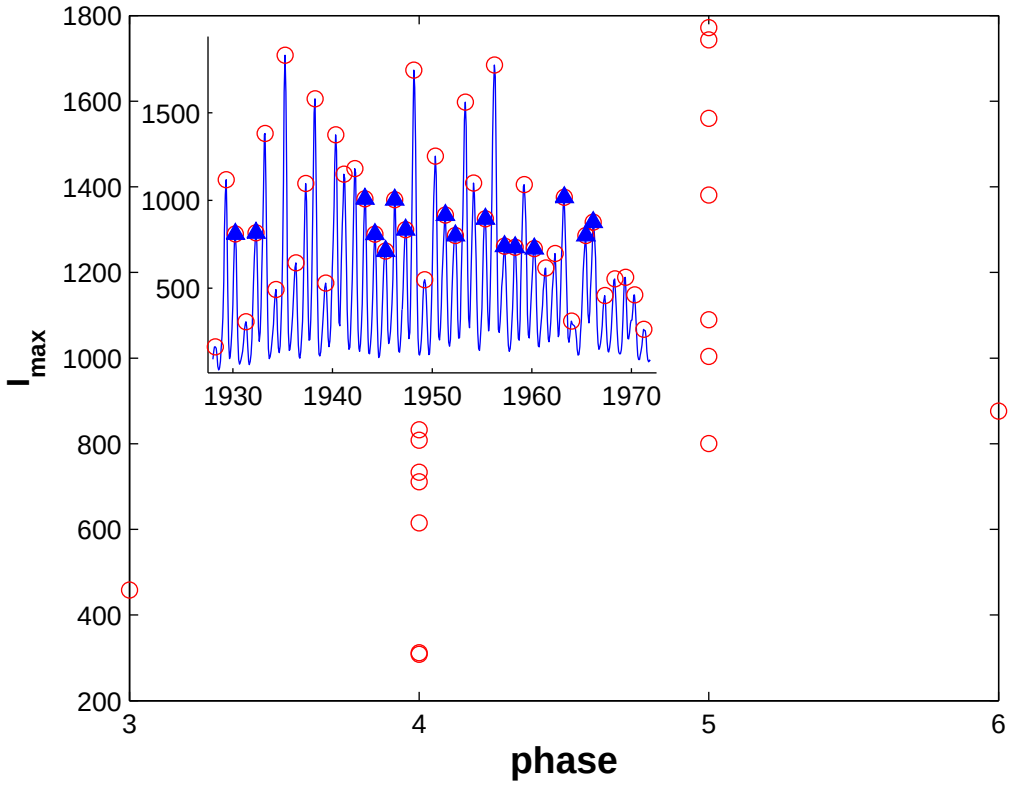

Figure 7: The relationship between an outbreak's *current phase* and the maximum number of mumps infectives in the *following year's* outbreak All intermediate sized epidemic peaks were collected marked with △ in the inset in the ranges (700:1050). New York mumps time series.

References and Notes

1. Engbert, R. and Drepper, F.R. Chance and chaos in population biology - models of recurrent epidemics and food chain dynamics. *Chaos, Solitons and Fractals*. **4,** 1147-1169 (1994).

2. May, R.M., Ferguson, N. M., and Anderson, R. M. In Spatial Ecology. Princeton University Press. 137-157. (1997)

3. Bjornstad, O.N. and Finkenstadt, B.F. and Grenfell, B.T. Dynamics of measles epidemics: estimating scaling of transmission rates using a time series SIR model *Ecol. Mono.*. **72,** 169-184 (2002).

4. Fine, P. E. M., & Clarkson, J. A. Measles in England and Wales-I:An analysis of factors underlying seasonal patterns. *Int. J. Epidemiol*. **11,** 15-25 (1982).

5. Fine, P. E. M., & Clarkson, J. A. Measles in England and Wales: An analysis of factors underlying seasonal patterns. *Int. J. Epidemiol*. **11,** 5-14 (1982).

6. Grenfell, B.T. and Bjornstad, O.N. and Finkenstadt, B.F. Dynamics of measles epidemics: scaling noise, determinism, and predictability with the TSIR model. *Ecol. Mono.*. **72,** 185-202 (2002).

7. Keeling, M.J. and Grenfell, B.T. Disease extinction and community size: modeling the persistence of measles. *Science.*. **275,** 65-67 (1997).

8. Kermack, W. O., & McKendrick, A. G. Contributions to the mathematical theory of epidemics. *Proc. Roy. Soc. A.* **115** 700-721 (1927).

9. London, W. P., & Yorke, J. A. Recurrent outbreaks of measles, chickenpox and mumps. 1. Seasonal variation in contact rates. *Am. J. Epidemiol*. **98,** 453-468 (1973).

10. Murray, J. D. Mathematical Biology. *Springer - Verlag Berlin*. (1989).

11. Xia, Y. and Bjornstad, O.N. and Grenfell, B.T. Measles Metapopulation Dynamics: A Gravty Model for Epidemiological Coupling and Dynamics *Am. Nat.*. **164,** 267-281 (2004).

12. Anderson, R. M., & R. M. May. *Infectious Diseases of Humans: Dynamics and Control* Oxford University Press, New York, (1991).

13. Henson, S. M., Cushing J. M., Costatino, R. F., Dennis, B., and Desharnais R. A. Phase switching in population cycles. *Proc. R. Soc. Lond. B.* **265,** 2229 (1998).

14. Olinky, R., Huppert, A. and Stone L. Thresholds in seasonally forced epidemiological models. (submitted). Olinky R. PhD thesis, Tel Aviv University (2005).